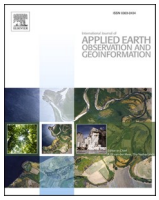
International Journal of Applied Earth Observations and Geoinformation 108 (2022) 102729



Contents lists available at ScienceDirect

International Journal of Applied Earth Observations and Geoinformation

journal homepage: www.elsevier.com/locate/jag



Investigating optimal unmanned aircraft systems flight plans for the detection of marine ingress

Ben Mcilwaine, Mónica Rivas Casado *, Toby Waine

School of Water, Energy and Environment, Cranfield University, College Road, Cranfield MK43 0AL, United Kingdom

ARTICLE INFO

Keywords:
Marine ingress
Optimisation
Flight search patterns
Remote sensing
VLOS EVLOS BVLOS
Unmanned aircraft systems

ABSTRACT

From the shutting down of coastal tourism industries, the mass destruction of aquaculture, to the clogging of power station water intakes, marine ingress events have the potential to cause widespread disruption along our coastlines. To gain the ability to respond to such events, efforts are being made to advance the understanding of bloom events which predominantly present as large aggregations of jellyfish, or detached aquatic macroalgaes in the water column. This paper investigates the optimal flight search patterns with a focus on marine ingress bloom detection from unmanned aircraft systems (UAS). The detection performance of four flight search patterns are examined against five different bloom shapes. Monte-Carlo simulations are deployed to assess probable performance of flight search pattern against variable bloom shapes. A total of 50,000 simulated flights were conducted, offering a maximum of 500 million marine ingress objects for possible detection. A two phased flight approach is proposed, with first phase flights conducted as area search strategies, and second phase flights as datum searches for scenarios where some information of possible bloom location is available. Parallel sweep was found to be the best performing generalist flight search pattern, closely followed by the phase two search pattern expanding square. Crossing barrier was found to be competitive but appeared to lend itself towards specific detection scenarios with sector search being a consistently poor performing flight search pattern. This paper also investigates the comparative performance of visual line of sight (VLOS), extended visual line of sight (EVLOS), and beyond visual line of sight (BVLOS) operations. Increase of total survey area was found to increase bloom detection frequency, with BVLOS operations the highest performer successfully increasing bloom detection by a factor of 3.7. This paper exhibits the first assessment of flight search patterns within the context of drone-based detection of marine ingress bloom events. This should facilitate the development of an early warning detection system that can provide reliable warning to coastal industries prior to a marine ingress event occurring.

1. Introduction

Coastal industries regularly battle with the 'marine ingress problem' (Purcell, 2005; Flynn and Chapra, 2014). Marine ingress predominantly forms as large aggregations of jellyfish and submerged aquatic vegetation (Lapointe and Bedford, 2007; Kim et al., 2012), although other less conspicuous forms do exist as well (Maclsaac, 1996). Coastal industries such as desalination plants and nuclear power stations often require large volumes of water to operate; water intakes at these coastal locations can get clogged during marine ingress events, resulting in reduced productivity (Kim et al., 2012). For example, losses of revenue for nuclear power stations can potentially reach up to US$ 1 million dollars per day per reactor (Nuclear Energy Institute, 2015; Kim et al., 2016). This leads to a conflict between the running of the coastal industry, and the source of the biological matter that contributes to recurrent ingress events. This is of particular concern when considering the ecological importance of seaweed and kelp bed habitats, and the relatively unknown ecological role played by many jellyfish species (Riascos et al., 2018). However, other industries such as tourism, sporting events, and fin-fish aquaculture are not immune from marine bloom events and can be impacted by the same difficulties (Zoltan et al., 2005; Lippmann et al., 2011; Haberlin et al., 2021). Marine ingress is essentially undesired biomass from the ocean that can potentially cause huge disruption for coastal industries, and is critically important within the marine environment due to this reality.

Barrier netting systems have proven to be useful for aquaculture and coastal tourism (Vasslides et al., 2018), but have to be carefully managed to prevent biofouling and damage (Klebert et al., 2013).

* Corresponding author.
E-mail address: m.rivas-casado@cranfield.ac.uk (M. Rivas Casado).

https://doi.org/10.1016/j.jag.2022.102729
Received 6 December 2021; Received in revised form 5 February 2022; Accepted 17 February 2022
Available online 8 March 2022
0303-2434/© 2022 The Authors. Published by Elsevier B.V. This is an open access article under the CC BY license (http://creativecommons.org/licenses/by/4.0/).

Nuclear power stations and desalination plants often utilise multi-stage filtration procedures within their cooling water intake systems. However, with larger marine ingress events these systems can be overloaded (Wei et al., 2018). With the provision of early warning of an impending ingress event, coastal operators can initiate damage mitigation techniques. Water intake rates can be reduced to levels where ingress debris can be processed by the inbuilt filtering systems. For more extreme volumes of marine ingress, an increased workforce can be brought onto site to assist the filtering systems by hosing down drum screens and removing excess biomass. Without prior warning, severe productivity-related delays can occur, leading to reduced site efficiency and potential damage to filtration systems (Kim et al., 2012).

Currently, there are minimal options to detect the source of marine ingress events before their occurrence. Even if detection is possible, their ability to provide a reliable warning of an impending event is not currently available. Several studies have focused on the detection of jellyfish using environmental DNA (eDNA), however difficulties in the longevity of DNA in the marine environment are well documented (Thomsen et al., 2012). eDNA is primarily used for the detection of genetic material presence but not necessarily the current location of a species individual which does not lend itself towards the application of an early warning system (Minamoto et al., 2017). Ecological forecasting models have found success in highlighting environmental conditions that are significant predictors of medusae presence (Decker et al., 2007) but are not intended to pinpoint an exact ground-truthed location as would be required for an early warning system. Aerial remote sensing attempts at jellyfish detection have taken place, providing variable success rates across methods ranging from unmanned aircraft systems (UAS) (Kim et al., 2015, 2016; Schaub et al., 2018), light-aircraft (Houghton et al., 2006) to satellites (Becking et al., 2015). Remote sensing efforts to date have predominantly been focused on the use of RGB sensors, regardless of remote sensing platform. Contrary to the statement by Jo et al. (2017) that monitoring jellyfish with imaging satellites is not possible, there have been successful attempts at detecting jellyfish blooms (Thorn and Lambert, 2016). We do, however, agree that satellites on their own are not an appropriate jellyfish ingress monitoring platform. Predominantly due to the time taken to orbit and in turn access data, their comparatively low-resolution images, and the remote sensing challenges they face concerning atmospheric water vapour (Li and Wu, 2021; Rogozovsky et al., 2021).

Marine ingress is frequently comprised of jellyfish-based events during summer, and submerged marine vegetation during winter months due to more stormy conditions leading to detachment of vegetation from their growing substate. Research focusing on the remote detection of the majority of marine vegetation is well established (Dierssen et al., 2015; Menu et al., 2021; Rowan and Kalacska, 2021). Seagrasses have been successfully detected and researched remotely for many years, with their sessile and high-density characteristics large contributors to the ease of detection. Despite not technically being vegetation, the remote sensing of microalgae blooms is also well documented due to their conspicuous nature, the tendency to form large blooms and their links to harmful algal blooms (HABs) (Weybright and Kelly, 2016; Kwon et al., 2020; Mardones et al., 2021). The toxins produced by microalgae blooms can cause reductions in habitat biodiversity by killing fish species and marine vertebrates through food chain biomagnification (Bricelj et al., 2012), but can also indiscriminately decimate groups of respiring animals due to their ability to induce hypoxic conditions (Hu et al., 2006; Mohd-Din et al., 2020). However, macroalgae blooms (MABs) are less well researched yet also have the potential to cause severe disruption to coastal industries (Gansel et al., 2017; Liu et al., 2020). MABs can form through large-scale detachment from their region of growth, or can also grow on the ocean surface; resulting in the suspension of large quantities of biomass in the water column (Marx et al., 2021). This biomass can often end up scattered across inter-tidal coastal habitats (Fig. 1). This transition from a stationary growing location to one of mobility in the water column is often the most frequent cause of clogging of water intakes at nuclear power stations.



Fig. 1. Example of a large section of macroalgae found in Cape Town, South Africa (Nov 2019).

The full economic, social and ecological impact of MABs in coastal regions is not well understood, but pressure from commercial industries has begun to change this (Thompson et al., 2020). Research into the monitoring of MABs, and an early warning system, has been previously called for (Mcilwaine et al., 2019) but due to their low density, non-sessile and varied depth nature, advances have been slow. To deal with the increasing global rates of MABs, efforts must focus on improving the remote sensing techniques to detect and study them. This will require a comprehensive understanding of all the aspects comprising an early warning remote sensing system, from the characterisation of the spectral signature to the detection capability of blooms in the marine environment. Recent work by Mcilwaine et al. (2019) identified the wavebands most appropriate for macroalgae marine ingress detection, and also presented the first multi-ocean, multi-sensor jellyfish bloom detection capability (Mcilwaine and Rivas Casado, 2021). Without the ability to reliably detect, there is no possibility of providing a warning before an ingress event occurs. This reliability of detection must be inherent in whatever technology is used to provide early warning of marine ingress, be it jellyfish or MAB based.

UAS have repeatedly been shown to have superior accessibility, resolution and price-performance balance compared to more traditional remote sensing techniques (Colomina and Molina, 2014; Schaub et al., 2018; Kwon et al., 2020). Especially as found by Mcilwaine and Rivas Casado (2021) who showcase UAS based remote sensing, combined with Artificial Intelligence (AI), as a highly successful method of jellyfish detection (>90% classification accuracy) in the context of requiring rapid data access. However, UAS based remote sensing technologies are not without their own challenges. Rain, wind speed, and flight duration limitations - in addition to local legal policy - all provide challenges to UAS operations (Albajes-Eizagirre et al., 2011; Nahirnick et al., 2019; APA, 2020). Recent advancements in UAS technology have allowed new research avenues to be explored, from the mapping and classification of ecologically sensitive marine habitats (Ventura et al., 2018) to the quantification of marine macro litter (Gonçalves et al., 2020) and Antarctic predators (Goebel et al., 2015). With a reliable platform for the

remote sensing of ingress events, a move towards the production of an early warning system becomes feasible.

To reliably detect and warn of inbound marine ingress events, UAS are the current best hope for prospective early warning schemes (Mcilwaine et al., 2019). However, due to their relative infancy there is no current framework, or structured guidance, in place for surveying the marine environment. In this paper, a conceptual framework that considers optimal survey routes, and takes into account the most common naturally occurring bloom shapes, is proposed. Bloom shape has the potential to highly impact the rate of successful detection with respect to the type of flight search pattern used, and it is vital to identify which search pattern can cope with the natural variability of the marine environment. Aircraft-based search and rescue efforts in the marine (and terrestrial) environments are well documented and transferable lessons can most certainly be applied to UAS based marine remote sensing. Optimisation of surveying routes is critical for any proposed operational framework to be successful (Auditorium and Washington, 1980). By both optimising and standardising survey effort (the anecdotal sum of survey duration, distance travelled and survey coverage), guidance for the early detection of marine ingress events could help provide the structure of a practical and workable early warning system. Many parameters can be altered to improve survey performance such as battery endurance, the type of the flight search pattern, but also how the overall mission is optimised for various shapes and sizes of marine ingress events. In some instances, satellite imagery can be obtained to ascertain bloom shape. However, if these data are not available, then detection can be gained from UAS flights at a desired location. Another question that would be beneficial to address; is there any advantage (to an early warning system) in optimising visual line of sight (VLOS), extended line of sight (EVLOS) and beyond visual line of sight (BVLOS) UAS operations. Through gaining the ability to fly further and even out of sight, additional avenues of potentially increased performance improve rapidly. This also in turn can allow reductions in the cost of flight operations. However, an increase in flying further is not a prerequisite for BVLOS flight. BVLOS operations can in theory include small-area surveys, with the defining factor being the pilot not having the ability to directly view the UAS themselves (Table 1).

The type of UAS operation (VLOS, EVLOS, BVLOS) has the potential to greatly impact ingress detection, assuming comparable flight parameters. Fig. 2 visualises the coverage between the three forms of operation: visual line of sight (VLOS), extended visual line of sight (EVLOS), and beyond visual line of sight (BVLOS). The key difference between the three forms of operations are predominantly changes in potential maximum survey area ('as the crow flies'), with substantial

Table 1
Definitions of Civil Aviation Authority (CAA) regulated operation types (based on CAP 722 8th edition (Civil Aviation Authority, 2020)).

Type of operation	CAA definition
Visual line of sight (VLOS)	The remote pilot must maintain clear sight of the UAS and surrounding area at all times during the operation. Any form of "image enhancing" devices such as binoculars are not permitted. The UAS must only be flown within the pilot's eyesight (maximum 500 m horizontal distance from the pilot).
Extended visual line of sight (EVLOS)	Technically a form of BVLOS operation. Requires authorisation from the CAA but is not location-specific. Like with VLOS operations, collision avoidance is conducted through "unaided visual observation". However, this is commonly mitigated by using additional observers dedicated to assisting the mission.
Beyond visual line of sight (BVLOS)	Any operations that are conducted at distances further than the pilot can directly view the UAS, and respond to and avoid other airspace users, with their own eyes. There is a requirement for mitigation that can prevent any threat of collision to aviation. CAA authorisation is mandatory and location-specific. Additional observers are not compulsory to conduct operations.

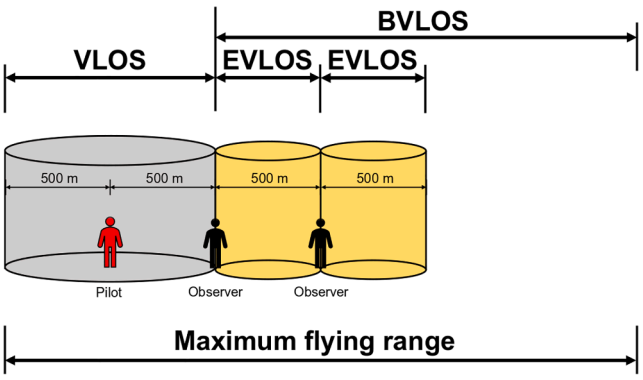


Fig. 2. Visual line of sight (VLOS), extended visual line of sight (EVLOS) and beyond visual line of sight (BVLOS) operational illustration.

operational differences regarding personnel for respective mission types. As the wider usage of UAS expands, and not just for remote sensing tasks, it is critical to maintain a grasp on the type of operation (VLOS/EVLOS/BVLOS) due to rapidly changing legal policy (Davies et al., 2018) that may enhance or limit usage. A robust early warning framework should account for both jellyfish and MABs to have success upon deployment.

The introduction of a framework for optimised UAS marine ingress detection would benefit a wide range of coastal industries; potentially prevent lasting damages and decrease marine ingress related reductions in productivity. An output of an optimised flight plan for a given operation type (VLOS, EVLOS, BVLOS) would be a significant improvement on current warning systems and operational procedures. Whilst also gaining the awareness of whether to apply a generalist approach or a situation-specific approach; this would be a huge benefit to the global battle against marine ingress. This paper aims to provide a conceptual framework that can provide the initial guidance for UAS marine ingress detection in the marine environment. This work hopes to become a practical tool that can be implemented by a wide range of coastal operators, not just one specific industry, and determine the most suitable flight plan for a given combination of bloom shape, bloom size, and flight search pattern. It should also complement the work in Mcilwaine and Rivas Casado (2021) where algorithms to detect marine ingress were developed using convolutional neural networks.

This study aims to contribute to the delivery of an optimised conceptual framework for the UAS detection of marine ingress events. This will be achieved through the following objectives:.

Assess the performance of various VLOS search patterns across the most commonly occurring bloom shapes.

1. Assess the performance of various VLOS search patterns across the most commonly occurring bloom shapes.
2. Quantify and explore the differences in detection performance of both VLOS, EVLOS and BVLOS flights.
3. Develop a conceptual decision support chart to quickly ascertain the optimum flight plan.

2. Materials and methods

2.1. Site selection

The framework was developed for the area surrounding Torness nuclear power station (East Lothian, UK) (Fig. 3). Torness nuclear power station is regularly affected by marine ingress and has water intake systems that are typical of other UK and global nuclear power stations and desalination plants. Torness is powered by two advanced gas-cooled reactors (AGR) with a water intake system consisting of large drum screens for filtration of debris. Each drum screen draws in large amounts

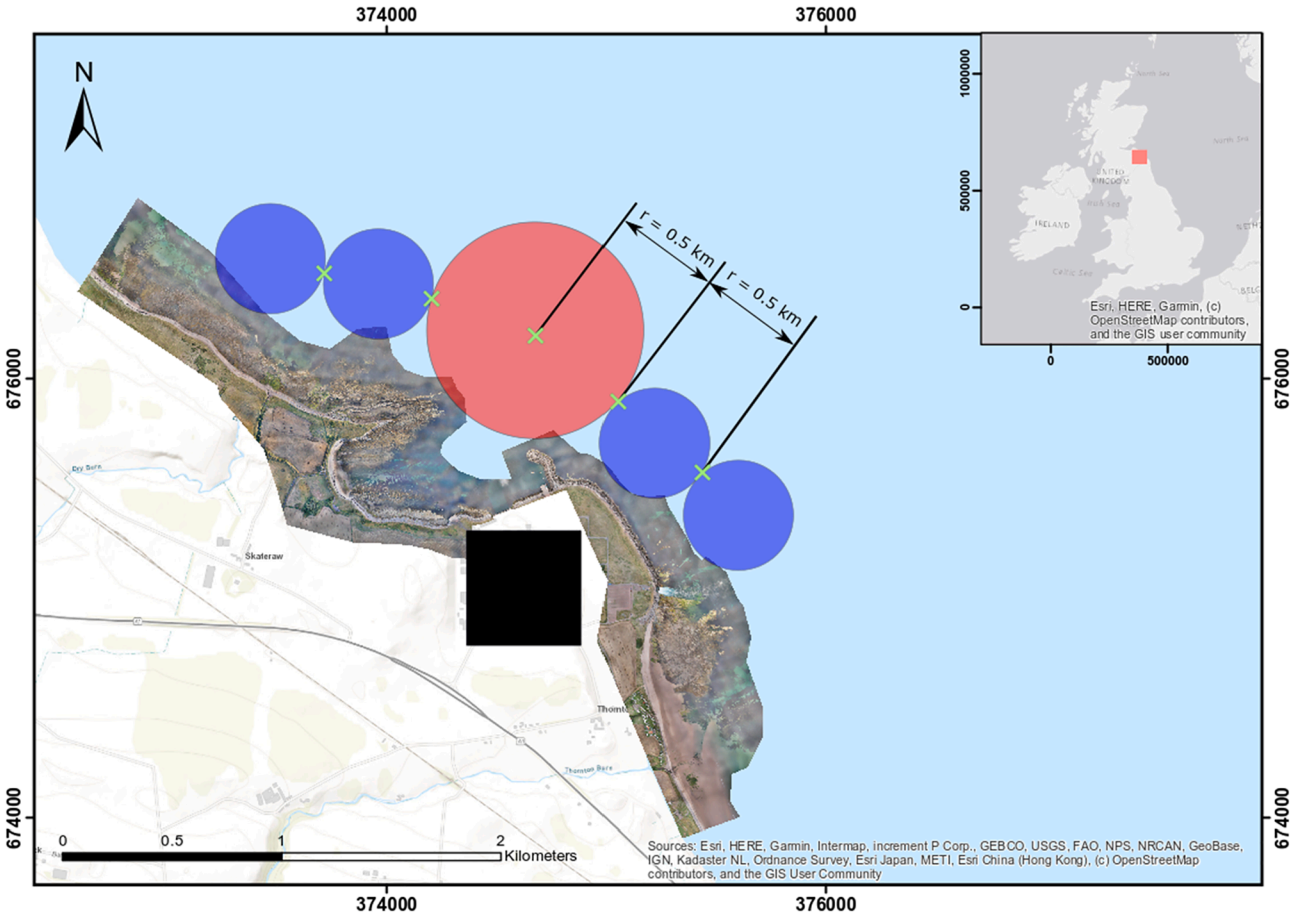


Fig. 3. In-situ depiction of Unmanned Aircraft Systems maximum operational capabilities using Torness nuclear power station, East Lothian, UK, as an example: black square = nuclear power station, red circle = Visual Line of Sight (VLOS), blue circles = Extended Visual Line of Sight (EVLOS) extensions. Beyond Visual Line of Sight (BVLOS) (not depicted) could theoretically expand indefinitely. Green crosses suggest possible positions of pilot/flight observers on boats, as is common practice for marine surveys. (For interpretation of the references to colour in this figure legend, the reader is referred to the web version of this article.)

of water from the ocean and has a direct impact on how much power the station can generate at a time (Chae et al., 2008).

Fig. 3 shows the zonation of the study area, with representative areas showing the theoretical maximum extent of VLOS, and EVLOS, flights. In turn, providing an easy-to-understand visual description of survey area coverage in relation to the water intake location.

2.2. Generation of data

Synthetic data were generated to simulate bloom shapes and flight search patterns. Within this context 'bloom shape' refers to the spatial composition of a generic marine ingress object, and flight 'search pattern' refers to the flight pattern that the UAS takes to survey an area when searching for a given marine ingress bloom. The analysis will be focused on optimising UAS flight plans, and makes no attempt at being able to discriminate between different types of marine ingress. Five distinct shapes of bloom were simulated to cover the most commonly occurring, natural bloom shapes; derived from imagery collected during jellyfish data collection flights conducted between 2016 and 2018. Despite being derived from jellyfish data, it is hoped that there are useful levels of transferability to macroalgae blooms. The bloom shapes investigated were as follows: 'large coverage', 'clustered', 'elongate' 'small coverage' and 'circular' (Fig. 4). The small coverage bloom shape looks unnatural in its representation, however is a common occurrence during bloom events due to the presence of anthropogenic structures (such as docks, jetties and piers). Each bloom, regardless of shape, consisted of 10,000 marine ingress objects to ensure equivalence of comparison when investigating search pattern performance. Blooms consisting of 10,000 objects were selected due to previous UAS imagery (greater than4,000 images) collected giving an indication of bloom extent; the same images were also used to develop JellyNet (Mcilwaine and Rivas Casado, 2021).

All bloom shapes were created by individually hard-coding each shape within individual bespoke 'R' scripts. The basis of bloom shape structure was built upon the principle of randomly filling matrix cells in relation to a designated cell position. Each script used a random distribution function to randomly fill cells within the shape matrix using the plot.matrix package. In order to maintain exactly 10,000 objects per bloom, each iteration of bloom was coded to over-fill each shape with bloom objects, with a secondary bespoke 'hunting' algorithm used to eliminate single bloom objects when blooms exceeded 10,000 objects (removal via the same random distribution function used to fill the blooms). This ensured each bloom had exactly 10,000 objects to allow a statistically robust and equal comparison across every iteration. This process had to be applied to all bloom shapes, and was essential due to the nature of the generation of randomised blooms, and in particular clustered shaped blooms; where a randomised number of clusters were generated, with a randomised number of bloom objects surrounding each cluster. This meant that in some instances, this would create bloom iterations of under or over 10,000 marine ingress objects. By ensuring bloom sizes were initially created marginally larger than 10,000 objects, and then trimmed down to a total bloom size of 10,000, equivalence was maintained for fair comparison across all bloom simulations. During the Monte-Carlo simulations, each of these bloom shape scripts were called

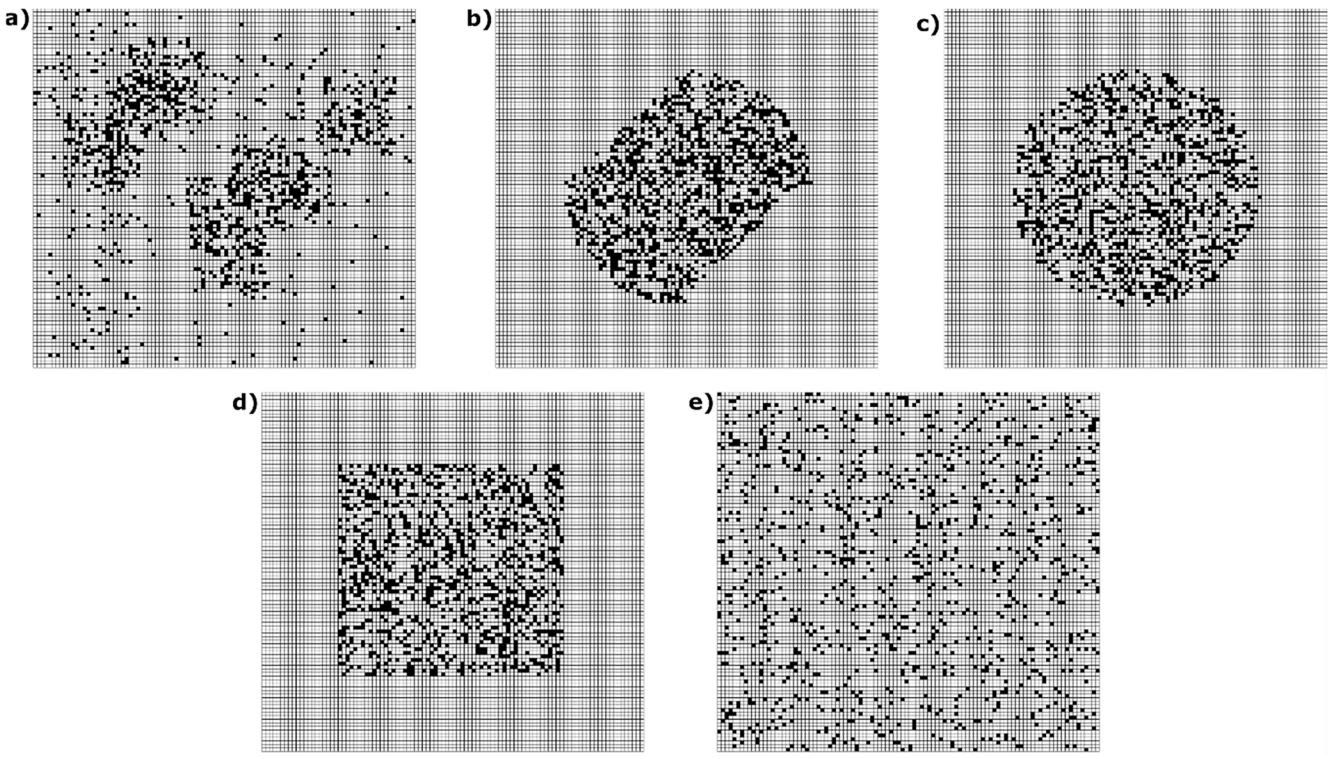


Fig. 4. Examples of investigated bloom shapes: (**a**) Clustered; (**b**) Elongate; (**c**) Circular; (**d**) Small coverage; (**e**) Large coverage. Each cell represents an area of 0.25 m × 0.25 m, with black marks indicating presence of a marine ingress object. The survey area is composed of 4,000 × 4,000 cells, therefore a total area of 1,000 × 1,000 m.

into the main simulation script as and when required.

Blooms were simulated within 4,000 × 4,000 cell matrices, with marine ingress objects represented by a binary value of presence or absence within a given cell. Each cell represented a real-world size of a common marine ingress object: an *Aurelia aurita* individual of 0.25 m diameter (Tombs, 2015), in turn defining a survey area of 1,000 × 1,000 m. Once the matrices were generated, marine ingress objects were then randomly populated within the desired bloom shape and iterated 1,000 times to complete their simulation cycle. Synthetic data generation for flight search patterns was based within the context of using a single generic UAS platform. This allowed representation of both fixed-wing, and multi-rotor platforms; the two most accessible and widely applicable UAS platforms (Simic Milas et al., 2018). Flight search pattern and bloom simulations were processed using a high-performance computer (HPC) with the following specifications: Dell Precision Tower 5810, Intel Xeon E5-1650 v4 CPU, NVIDIA GeForce GTX 1080 GPU and 64 GB of RAM.

A flight altitude of 100 m was assumed; providing the basis of image collection for each iteration of every flight scenario. As a consequence, the image field of view was 18 × 18 m (found to be a realistic image chip size) based on the real world flights conducted by Mcilwaine and Rivas Casado (2021). This would equate to a ground sampling distance of 1.63 cm/px if using a common imager like a Sony Alpha a6000 mirrorless RGB sensor (sensor: 23.5 × 15.6 mm, resolution: 24.3 MP 6,000 × 4,000) (Sony, 2021). Simulations were run within the statistical software R 3.4.3 (R Foundation of Statistical Computing, Vienna, Austria) (R Core Team, 2017) with the following packages: 'ggplot2' and 'plot.matrix'. Flight simulations, for each unique combination of bloom shape and flight search pattern (scenario), were generated and iterated 1,000 times (Fig. 5). This was conducted to provide a more realistic representation of uncertainty when working with regional risk assessment simulations for the marine environment (Hayes and Landis, 2004).

Flight search pattern simulations were categorised into two phases. Phase 1: no information is currently known on the location of the bloom. Phase 2: some level of information is currently known as to the location of a bloom. These are sometimes referred to as an 'area search' (phase 1) or 'datum search' (phase 2). The reference of two phases is due to the context of investigating optimum flight search patterns for the detection of marine ingress for an early warning system. When there is no current information on bloom locality, then an area search (phase 1) should be deployed. However, when a successful locating of marine ingress has occurred during previous flights, subsequent flights should deploy a datum search (phase 2) as a matter of priority. This split was conducted to maintain alignment with well-established search techniques for maritime search and rescue efforts (Royal National Lifeboat Institution, 2017). Phase 1 search patterns used were parallel sweep, and crossing barrier; phase 2 search patterns consisted of expanding square search, and sector search (Fig. 6). Phase 2 searches were initiated from a random ingress presence location within the simulated bloom, per iteration. Crossing barrier and sector search are both examples of repetitive flight search patterns; all four flight search patterns captured the same number of simulated images to ensure equivalence of survey effort across all flight search patterns. The performance of phase 1 and phase 2 flight search patterns were evaluated independently- i.e., simulations for phase 2 were not linked to phase 1 simulations.

2.3. Investigation of optimised flight plans

The primary output of the flight search pattern simulations were frequency counts of successful marine ingress detection within the simulated image capture area. The total counts of the simulations resulted in 1,000 individual frequency tallies per scenario; each unique combination of bloom shape and flight search pattern. The count of ingress detection was tallied through the flight search pattern over the bloom. With each iteration producing 10,000 marine ingress objects, a total of 200 million marine ingress objects were available for detection through the initial simulated flight search patterns. The median detection rate for each scenario is reported, across all iterations, along with

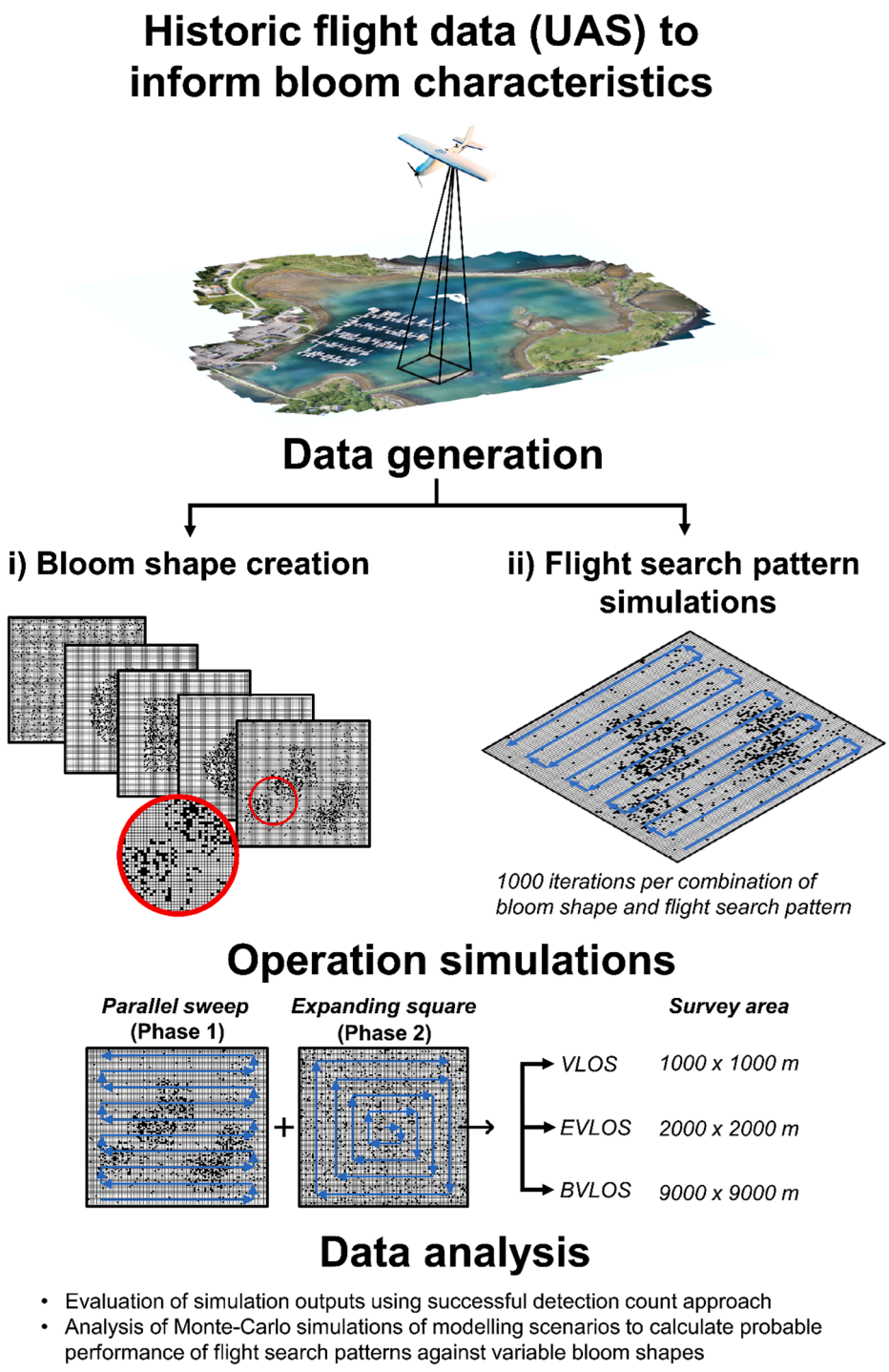


Fig. 5. Overall work-flow diagram summarising the methodological processes: using historic Unmanned Aircraft Systems flight images to provide information on bloom characteristics; generation of data for the five assessed blooms and four flight search patterns, and associated flight simulations; operational investigation using the best performing phase 1 and phase 2 flight search patterns and associated flight simulations; analysis of simulations outputs.

the respective standard deviation (Table 2). This was completed to provide a more representative indication of central tendency across the scenario distributions, and their respective simulation iterations. This was conducted due to the output data being count data, and therefore an increased likelihood of skewness.

The count frequency distributions were collated into multiple box-plots to show both the variance and nature of each of the 20 unique scenarios with respect to each flight search pattern. This was conducted to provide insight and context to the range of flight search pattern performance (flights) across all 1,000 iterations per scenario. In turn, also providing information on the performance of each flight search pattern across the bloom types that were available for survey. There is currently no formal definition of what substantiates a bloom. The threshold value (*beta*) used to initiate a response to detection of marine ingress was selected at 50 counts per survey flight; with a field of view of 18 × 18 m, equating to 50 images containing a minimum of at least one marine ingress object (and highly likely many more) in 900 linear metres of survey. In the situation of a marine ingress bloom being present, this would certainly involve an amount of ingress that could cause moderate to severe disruption to coastal industries. From this point on,

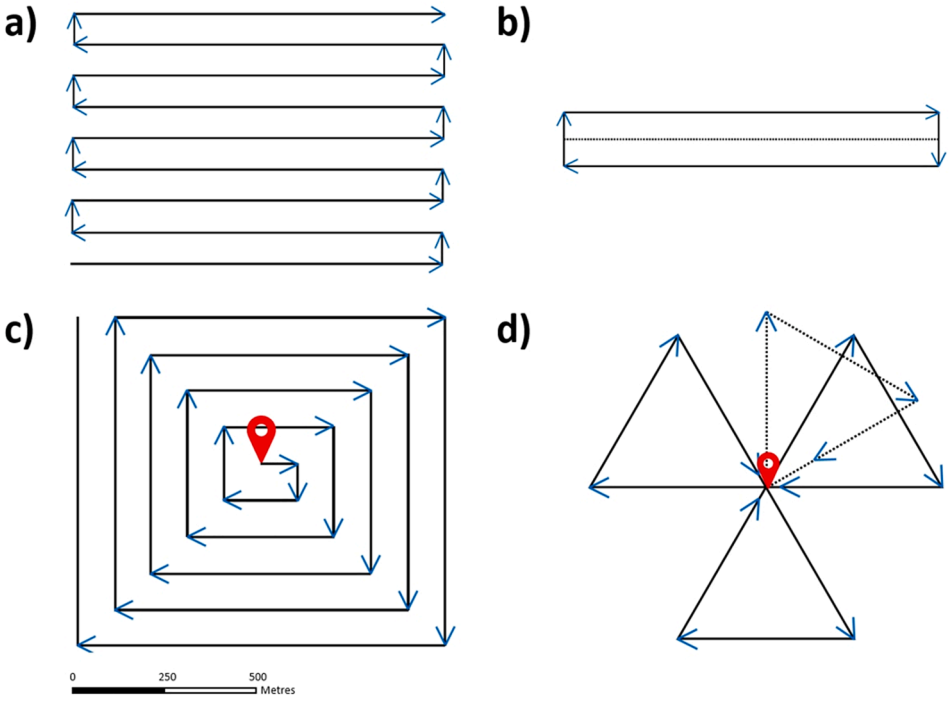


Fig. 6. Investigated flight search patterns: phase 1 = (**a**) Parallel sweep; (**b**) crossing barrier; phase 2 = (**c**) expanding square; (**d**) sector search. Red pin indicates datum for phase 2 flights. (For interpretation of the references to colour in this figure legend, the reader is referred to the web version of this article.)

Table 2
Median detection rate of marine ingress simulations per scenario, per 1,000 replicates. Frequency tally of detection with standard deviation in brackets.

			Bloom Shape				
			'Large coverage'	*'Clustered'*	*'Elongate'*	*'Small coverage'*	*'Circular'*
Flight search pattern	Phase 1	*Parallel sweep*	85 (7.4)	95 (6.7)	96 (3.1)	107 (4.7)	108 (4.3)
	(area searches)	*Crossing barrier*	32 (10.0)	44 (18.8)	88 (6.5)	76 (7.8)	84 (9.4)
	Phase 2	*Expanding square*	64 (6.6)	86 (7.2)	96 (3.1)	106 (4.6)	108 (4.4)
	(datum searches)	*Sector search*	8 (2.6)	10 (3.7)	15 (1.6)	17 (2.0)	19 (2.1)

this threshold will be referred to as the "*beta* threshold" value.

2.4. Impact of operation type

By building on the results from flight plan optimisation (Section 2.3), we were able to explore and quantify the effect of changing operation type (VLOS, EVLOS, BVLOS) on the rate of success of bloom detection. Only the best performing flight search patterns identified in previous sections (per phase) were included in the assessment of the operation type. Flight search pattern and bloom simulations were conducted with the same simulation constants as previously stated. However, the total possible survey area increased with respect to operation. Maximum possible survey areas were as follows: VLOS = 1,000 × 1,000 m, EVLOS = 2,000 × 2,000 m, BVLOS = 9,000 × 9,000 m.

3. Results

3.1. Investigation of optimum flight plans

The rate of detection for all configurations of flight search patterns and bloom shapes (Table 2) are for VLOS operation flight bounds. For every form of bloom shape, parallel sweep was the highest performing phase 1 survey style, but also overall flight search pattern. Crossing barrier was similar in performance to parallel sweep for both 'elongate' (88) and 'circular' (84) shaped blooms, but particularly struggled with 'large coverage' (32) and 'clustered' (44) blooms. Expanding square was

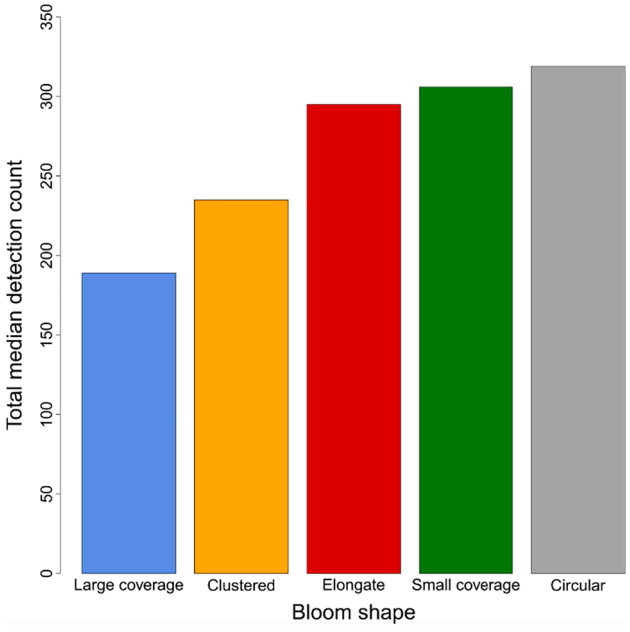


Fig. 7. The impact of bloom shape on detection performance, depicted using the sum of median counts for each iterated flight search pattern scenario with respect to bloom shape.

the best performing phase 2 search style by a significant margin across all bloom shapes. Much in the same way as crossing barrier, sector search struggled most with 'large coverage' (8) and 'clustered' (10) blooms, but unlike crossing barrier, it also struggled with 'elongate' blooms (15).

The best performing phase 1 search style for 'circular' shaped blooms was parallel sweep (108), closely followed by crossing barrier (84). Expanding square (phase 2) was an equally high performing search style for 'circular' blooms (108), however sector search severely struggled to reliably detect (19) in comparison to the other three survey styles. Despite this differential, sector search also struggled to detect well on all shapes of bloom, with it performing best on 'circular' blooms (19). 'Large coverage' shaped blooms were the hardest to detect with respect to flight search pattern, with parallel sweep (85) and expanding square (64) being the clear leading styles respectively. This finding of best-performing survey styles was the same case for 'small coverage' blooms however with more competitive performance for phase 1 with crossing barrier (76) versus parallel sweep (107). Much like low-density blooms, 'elongate' blooms were most easily detected using parallel sweep (96 (phase 1)) and expanding square (96 (phase 2)) with crossing barrier also performing well (88).

Across all four forms of survey style combined, there was a clear pattern in ease of detection with respect to bloom shape (Fig. 7). The bloom shape 'large coverage' had the lowest total median detection count of 189, with 'circular' having the highest with 319. Despite all replicates and simulations of bloom shapes maintaining the same number of marine ingress objects (10,000), bloom shape appears to significantly impact the success rate of marine ingress object detection. Fig. 8 shows the variability of counts for all 1,000 iterations of all 20 scenarios. Crossing barrier was hugely variable in detection performance, most notably for 'clustered' and 'large coverage' blooms. Parallel sweep was the most consistent performer across all bloom shapes, whilst simultaneously maintaining the highest detection performance across all five bloom shapes. Sector search had notably low variability in detection of marine ingress, however was also the worst-performing flight search pattern by a significant amount. Sector search was well below the designated performance threshold of 50 counts per flight, for all bloom shapes. The highest performing sector search iteration, of all

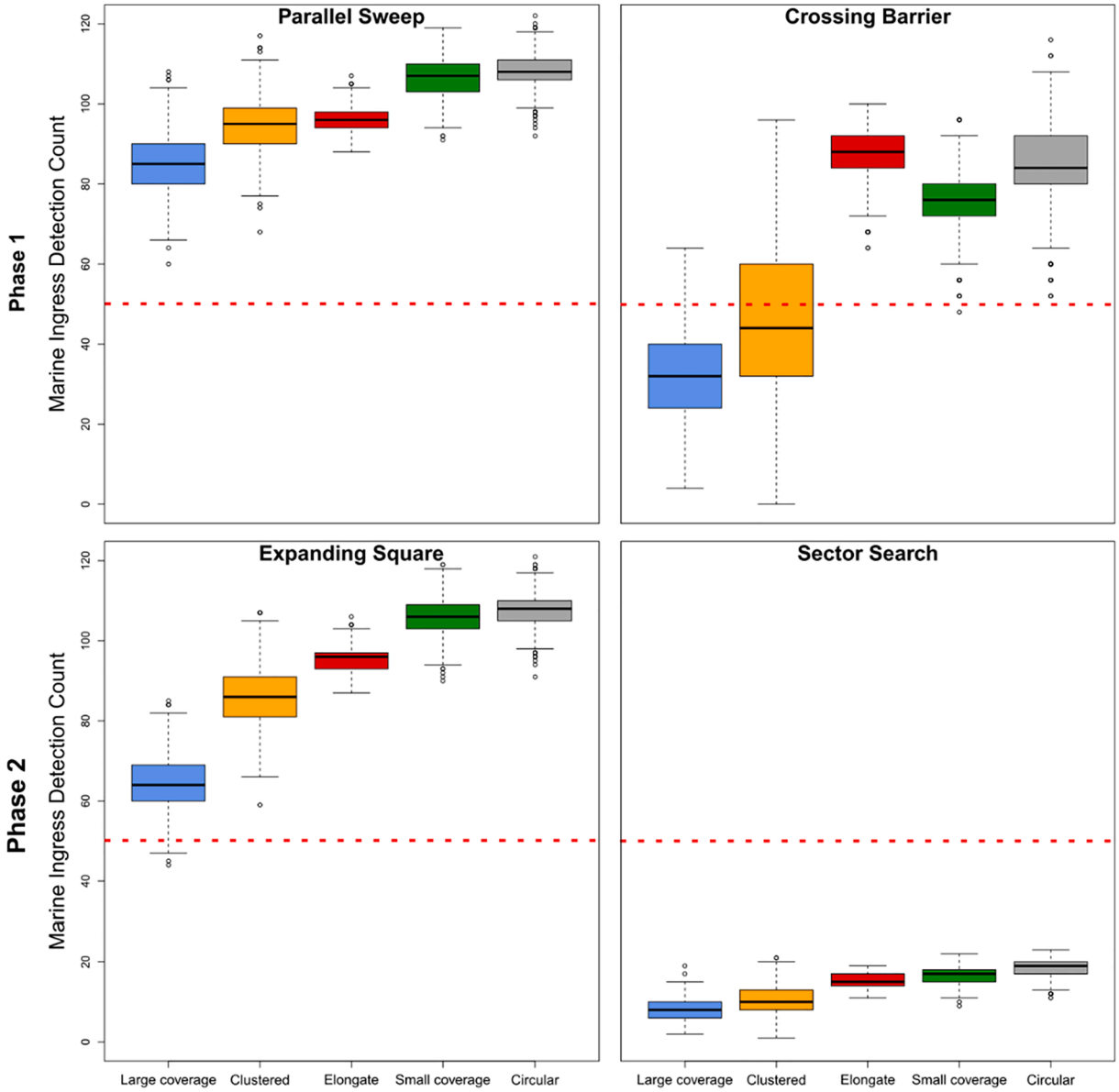


Fig. 8. Count data variance and structure across all 1,000 iterations for each unique pairing of flight search pattern and bloom shape. *Beta* threshold indicated by red dashed line. (For interpretation of the references to colour in this figure legend, the reader is referred to the web version of this article.)

5,000 iterations, occurred for a circular shaped bloom.

All four flight search patterns show the same general pattern in detection performance versus bloom shape. From hardest to easiest detection, this was 'large coverage; 'clustered'; 'elongate'; 'small coverage'; and finally 'circular' being the easiest to detect. The single exception to this trend occurred within crossing barrier simulations, in which there was a marked improvement in performance on 'elongate' blooms, and uniquely (versus other flight search patterns) had the highest median detection performance for 'elongate' blooms as well. The highest levels of variability per combination of flight search pattern and bloom shape occurred for crossing barrier; 'large coverage' and 'clustered' bloom shapes showed the largest ranges of performance across iterations, with 'clustered' bloom shape iterations ranging from detecting zero evidence of marine ingress objects to 96 detection events in a single flight. The median detection values for both of these scenarios fell below the threshold value of 50 confirmed detection images. Crossing barrier performed much better for the remaining three bloom shapes, with over 90% of all iterations performing above the threshold *beta* value. Despite this, crossing barrier remained the most inconsistent performer of all four flight search patterns.

Parallel sweep was the highest performer of all four flight search patterns, and the only flight search pattern with all 5,000 iterations above the threshold *beta* value. Variability of performance across all bloom shapes was only bettered by that of sector search, showing evidence of a consistently high performing generalist flight search pattern. Expanding square was very competitive with respect to parallel sweep, however performed worse on 'large coverage' blooms. Some iterations for the expanding square/'large coverage' scenario were not above the threshold *beta* value, however only a very small proportion (<1%). Within the context of survey phases, parallel sweep was by far the best phase 1 performing flight search pattern, and expanding square beating sector search for the best performing phase 2 flight search pattern. 'Clustered' blooms were the most variable in detect-ability, with 'elongate' blooms the most consistent in detection across all four search flight patterns. Despite not being a primary concern of the work, it is interesting to note the success of expanding square versus parallel sweep. Phase 2 flight search patterns should (in theory) be inherently lower performers due to the added variability of initiation of survey origin.

3.2. Impact of operation type on flight plan performance

Building on the findings of Section 3.1, parallel sweep and expanding square search were selected as the chosen phase 1 and 2 survey styles (Table 3). Operation type performance was assessed to include all five shapes of bloom per operation type.

VLOS operations had a sum median detection rate of 882 across both survey phases and all five bloom shapes. EVLOS operation flights had an increased detection rate with 1,709 (by a factor of 1.94), with BVLOS flights having the highest detection rate of all 3 operation types (3,253). BVLOS operations had exactly nine times more potential theoretical maximum survey area compared to VLOS and produced an increase in detection rate by a factor of 3.69 times.

4. Discussion

Marine ingress blooms have the potential to devastate the productivity of a diverse range of coastal industries (Matsumura et al., 2005; Barath Kumar et al., 2017; Vaughan, 2018). Marine ingress mainly forms as one of two types of biomass from the ocean: jellyfish or detached macroalgaes. Due to their sub-surface nature, relatively little is known about what can initiate specific blooms, with jellyfish blooms being the least well understood (Mcilwaine et al., 2019). Macroalgae blooms (MABs) are easier to locate due to their more simplistic pathway to suspension in the water column, but more research into their relationship with inclement weather systems would be hugely beneficial to the sector to ascertain causes of large-scale detachment from growing positions and vast increases in biomass growth. This research focused on five distinct bloom shapes, that are relevant for both jellyfish and MABs, and served as the spatial basis of variance within the conducted simulations. By iterating simulations over all five types of shapes simultaneously, any shape specific performance correlations were collected and then collated within survey performance output. In the field, it is likely that blooms are not strictly of one shape, but a blend of a few as imaged by Schaub et al. (2018); Mcilwaine and Rivas Casado (2021). However, for the purposes of quantifying the performance of different survey patterns with respect to bloom shape, this level of shape complexity was not required. This approach also allowed an indication of flight search pattern performance for general deployment across a range of shapes.

The outputs of the investigation into optimal flight plans were incredibly distinct with regard to the highest performing survey styles. For phase 1 survey styles, parallel sweep was by far the best and most consistent performer in detecting marine ingress objects. This is in congruence with what is found by marine search and rescue teams (Royal National Lifeboat Institution, 2017) and for the context of UAS surveying in the marine environment, is beneficial to know. Parallel sweep is an efficient and systematic area search, and for all shapes and forms of bloom, it performed the best. An argument could be made to deploy this form of survey route regardless of any other situational knowledge, and detection performance would likely be of practical use. Crossing barrier, in contrast, is structurally a very different search pattern (slidetodoc, 2021) and is originally intended for more niche area search demands. However, this does not mean it is limited to this usage. Predominantly meant as a repetitive curtain style search pattern to guard inlets and bays, the randomisation during the simulation process allowed an accurate and reliable performance measurement in such a way that ingress objects in the field would pass through the survey pattern's proverbial 'curtain'. Nonetheless, it was somewhat surprising to see just how well crossing barrier performed for both 'circular' and 'elongate' shaped blooms. This is particularly enlightening concerning flight mission planning, crossing barrier is the most accessible and simplistic of all investigated. If a rapid response is required, there may be some value in quickly deploying a crossing barrier survey style (slidetodoc, 2021). A caveat to this approach though, is that it was not a good performer across all shapes and would likely require ground-truthing before deployment; thus leading to the natural question that if ground-truthing has already occurred, then a phase 2 (datum search) would be a more logical approach. If crossing barrier was to be deployed against 'large coverage' or 'clustered' bloom shapes, the source of reduced performance is likely due to the more linear search area flown unlike the greater area coverage of parallel sweep. It is hard to avoid the broad-spectrum high-performance output of parallel sweep as, not just a phase 1 search pattern, but as a search pattern for any given bloom shape or phase of survey for a prospective marine ingress warning system. Despite the presence of many 90° corners within the search patterns (Fig. 6), it was assumed that UAS can follow the pre-planned routes with sub-metre accuracy, especially in the context of modern advancements in flight control software allowing far superior precision (Benassi et al., 2017). Any deviations from this path, more likely from fixed-wing platforms as opposed to rotary UAS, should be well overshadowed by the much larger coverage of the imaging field of view.

Phase 2 search styles were equally as conclusive as the outputs for phase 1; expanding square being the stand-out performer, and sector search only getting slightly under 20% of the detection performance (of expanding square search) for certain bloom shapes ('circular' & 'small coverage'). A note of particular resonance is how well expanding square search did with respect to parallel sweep (phase 1). Both phase 2 search styles began their data collection from randomised points within the bloom. This was to simulate field scenarios in which some information is known regarding bloom location, but not necessarily more than one field of view's worth of ingress accumulation coverage (18 × 18 m). Naturally, there will have been a portion of simulated phase 2 flight iterations centred over the edge of blooms, spending a significant portion of data

Table 3
Median detection rate of marine ingress simulations per operation type, for 1,000 replicates per bloom shape. Using the highest two performing flight search patterns. Sum of median frequency counts across all shapes of bloom per operation type.

		Operation type		
	Bloom shape	*VLOS*	*EVLOS*	*BVLOS*
Phase 1 (Parallel sweep)	Large coverage	76 (7.1)	106 (9.0)	136 (11.3)
	Clustered	90 (6.5)	185 (19.0)	425 (78.8)
	Elongate	94 (3.0)	220 (8.9)	469 (19.2)
	Small coverage	85 (5.5)	175 (9.8)	346 (16.9)
	Circular	111 (6.2)	178 (10.5)	256 (15.2)
	Phase 1 total	456	864	1,632
Phase 2 (Expanding square)	Large coverage	59 (6.3)	94 (8.6)	132 (11.2)
	Clustered	81 (6.7)	180 (19.9)	424 (79.1)
	Elongate	93 (3.1)	219 (8.6)	463 (19.5)
	Small coverage	84 (5.6)	175 (9.7)	344 (17.0)
	Circular	109 (6.0)	177 (10.3)	258 (15.4)
	Phase 2 total	426	845	1,621
	Grand total	882	1,709	3,253

collection time 'missing' that given bloom. It is hoped that with performance reporting focused on median values, the reporting of these situations were not overly influential, however it would not be unreasonable to assume it had some level of impact on the reduction of performance versus parallel sweep. This leads us to the next question, is it even worth splitting the flights into two distinct phases? By initiating phase 2 surveys on prior spatial location information, it is logically sound to commence data collection at such locations. Despite the decrease in overall detection performance, potentially by commencing phase 2 flights in such a manner, phase 2 style flights would have an underlying yet unquantifiable increase in the assurance of improving current information on a given bloom. Within the context of an early warning system, this is incredibly useful for any surveys conducted. In light of the above, and with expanding square within 1% of the performance of parallel sweep for three out of five bloom shapes, it is hard to deny the legitimacy of a double phased survey approach. On the other hand, sector search was significantly poor with regard to detection success, with it performing best on 'circular' shaped blooms (19), and worst on 'large coverage' (8). With a total median count (across all bloom shapes) of 69, equating to 15% of the capability of 'expanding square', it is clear that the 'sector search' survey style does not translate well to UAS surveying in the marine environment. This is likely due to sector search surveys originally being developed for surveying craft with a much larger field of view than a remote sensing UAS platform (Royal National Lifeboat Institution, 2017), and requiring more refinement to be translated as a UAS flight search pattern.

The *beta* threshold of 50 was developed in response to previous knowledge of UAS surveying in the marine environment, and coming to a threshold with a realistically low probability of a false positive in the field. There are no widespread formal definitions of what constitutes a bloom (Mcilwaine and Rivas Casado, 2021), however regardless of this, the definition used in this work was used primarily for analytical reasons; particularly within a decision making context of an early warning system. Further work is recommended to refine this threshold value, however naturally as a comparative value it would be not necessarily become more or less valid. The topic raises the broader question: at which point should a given coastal industry decide to react from warning provided via bloom detection. Does one single image detection of a bloom warrant an active response? Most likely not, but most certainly the *beta* threshold of 50 used here would do so. The percentage accuracy of the detection algorithm aspect of an early warning system also plays an important role here in the overall system. For a highly valuable coastal asset, would even one detection result be worth further investigation? Despite not being the focus of this work, it is also worth mentioning the pros and cons of false positives and false negatives of an early warning system. A false positive would be far more acceptable for all industries in comparison to a false negative, due to the huge potential impact of a marine ingress event. Dependent on the sensitivity of a coastal industry, they may wish to lower the *beta* threshold value in order to reduce the risk of false-negative action, or lack thereof.

Using a *beta* threshold of 50, seven of the 20 scenarios (Fig. 8) had a large number of flight iterations that were either straddling, or below the *beta* threshold value. These flight search patterns could not be recommended for use; especially in light of the consistently high performance of both parallel sweep and expanding square. Sector search for all bloom shapes was a very low performer and is not of any particular value in the context of an UAS early warning system. The uniquely elevated performance of crossing barrier on 'elongate' blooms is likely due to spatial compatibility of both the shape and the flight search pattern. This suggests potential use of crossing barrier for areas of interest with narrow inlets, elongated man-made structures such as large docks, or other narrow waterways. Unlike sector search, there may be some value in further investigation of this finding due to the simplicity of crossing barrier deployment. Despite not lending itself as a strong generalist performer, crossing barrier does appear to have merit for certain specific circumstances. Parallel sweep was the highest performer of all four flight search patterns, without a single iteration of all 5,000 falling below the *beta* threshold. For reliability of a deployed flight search pattern, consistency is most certainly a requirement. Despite parallel sweep not being the most consistent flight search pattern, it was only beaten in consistency of detection by the poorly performing sector search flights. The phase 2 flight search pattern expanding square was almost as good a generalist performer as parallel search. With the naturally occurring additional randomisation of a phase 2 flight, this result is worthy of recommendation as a practical flight search pattern. With regard to performance relating to bloom shape, there should be little surprise that 'clustered' blooms were the most variable to detect compared to other shapes; purely from a spatial randomisation point of view. Interestingly 'elongate' blooms were the most consistently detectable blooms, which may be in part due to their stretched spatial distribution. If a flight search pattern were to detect either end of an 'elongate' bloom, it is highly likely it would continue on to confirm detection of the rest of it.

BVLOS survey areas, unlike VLOS and EVLOS, are not precisely determined distances through civil aviation authority (CAA) guidance but are specifically granted for justifiable reasons on a case by case basis. A BVLOS area of 9,000 × 9,000 m was used following the author's BVLOS application (CAA, 2021a) for other project work on the east coast of Scotland, UK. However, a BVLOS maximum survey area could theoretically be smaller or larger than 9,000 × 9,000 m and is uniquely specific for each BVLOS application. It is frequent, however, when going to the administrative effort of making a BVLOS application, that a sizeable flying area is to be obtained. In UK airspace, as governed by the CAA, VLOS and EVLOS operations are of fixed maximum area coverage and relatively easy to conduct. BVLOS, however, are bespoke designated areas and can be viewed as more than just an extension of EVLOS operations. The first BVLOS authorisation was reported as being granted in April 2021 (CAA, 2021b), and our survey size of 9,000 × 9,000 m is based upon our own BVLOS application to fly on the east coast of Scotland as part of the UK government pathfinder project (Catapult, 2020).

The re-running of simulations to investigate the impact of operation type (VLOS, EVLOS and BVLOS) was highly successful in deciphering the broad-spectrum impact of the flying operation. Median counts of

individual bloom shapes were collated across the 5,000 total iterations, per phase, per operation type: a total of 30,000 blooms were analysed and assessed for the two selected survey styles (parallel sweep & expanding square – Table 3). The total median count for both survey phases (combined) were lowest for VLOS (882), followed by EVLOS (1,709) and then BVLOS (3,253). These results are to be expected in light of each operation type having an increasingly larger area of survey, in particular BVLOS with almost four times the detection rate of VLOS operations. EVLOS operations had an increase in detection capability of just under 93.7% compared to VLOS, as a result of doubling the theoretical total survey area to 2,000 × 2,000 m.

BVLOS operations are extremely rare in the UK and are at the cutting edge of the progression of UAS operational technology both nationally, and globally (Davies et al., 2018). The total number of civilian BVLOS operations in the UK (as of July 2021) is expected to be below five. Whilst guidance and operational protocol catch up with platform advancements, BVLOS operations remain practically inaccessible for the vast majority of operators. However, if the aim for BVLOS is purely to increase operational area, EVLOS could provide the solution. EVLOS operations are not limited to 2,000 × 2,000 m as investigated here. An EVLOS operation of this size assumes 2–4 dedicated flight spotters assisting the mission, but in theory, this could be extended to greater distances (and by virtue, area).

Truly distinct from both VLOS and EVLOS operations, BVLOS flights can be conducted without any direct visual contact between the pilot and the UAS (Civil Aviation Authority, 2020). BVLOS operations are not solely limited to attempts to increase the maximum theoretical survey area. In theory, a BVLOS operations area could be much smaller than that of a VLOS or EVLOS operation, but at a further distance from the pilot. BVLOS operations are generally more cost-effective (Fig. 10) due to being able to cover more ground, but also by being more efficient through requiring less take-off and landing manoeuvres. This reduces the demand on both UAS flight time and administration efforts in pre-flight planning. No spotters are required to conduct BVLOS operations, which also vastly reduces cost due to less personnel needed on the ground. In turn, these reasons have the potential to maximise surveying efforts in the marine environment and thereby the probability of collecting useful data at the survey location. BVLOS operations present a better survey area coverage per unit day cost in comparison to both VLOS and EVLOS. With the increase in potential survey area of BVLOS operations, aerodynamic optimisation of UAS platforms becomes much more critical as a flight variable. The scale of BVLOS search areas often means that multiple flights may have to be conducted, with battery capacity of the chosen platform being the limiting factor in how long a survey can be conducted for. This in turn leads to the rise in importance of how aerodynamic a flight platform is, especially for certain UAS platforms where battery capacity is fixed and can not be improved. The aerodynamic efficiency of a flying craft is normally described by the lift (L) to drag (D) ratio.

$$AE = \frac{L}{D}$$

where:

$AE = Aerodynamic\ Efficiency$
$L = Lift$
$D = Drag$

Fixed wing UAS platforms often have vastly superior aerodynamic efficiency in comparison to rotary platforms, and can cover much further distances due to this. The optimisation of the aerodynamic efficiency is commonly conducted by UAS manufacturers during production, however recent research is currently being conducted assessing this independent of private commercial industry (Di Luca et al., 2020; Panagiotou and Yakinthos, 2020; Zhu et al., 2020).

All early warning systems should at minimum consider the advantages and disadvantages of the nature of the deployed strategy. In particular, whether a generalist or specialist approach is superior. The best generalist performing phase 1 search pattern was found to be parallel sweep (total median detection count = 491 (Fig. 9), with expanding square (460) for phase 2 searches. Due to how competitively 'expanding square' performs compared to parallel search for 'circular', 'small coverage, and 'elongate'; it would be advisable to strongly consider expanding square as an alternative phase 1 survey style. If using expanding square as a generalist approach, or even as a phase 1 survey, consideration should be given to the starting point of the survey. Unlike a datum search, one would be committed to initialising a survey from the central point of the designated survey area in the absence of information of bloom location. There was no clear evidence of any benefit in using a survey style other than parallel sweep as a generalist approach, or in fact any other survey style, as a specialist approach for a specific bloom shape (disregarding a phased approach). This suggests that a repetitive flight programme would be most beneficial, repeating a phase 1 flight consisting of a parallel sweep area search, and then in the situation of locating a bloom, switching to a phase 2 datum survey consisting of expanding search.

A notable limitation of the simulations is the homogeneous nature of the simulation cells; the location where a marine ingress object may, or may not, have been located. All cells were of identical size and did not account for the heterogeneous sizes of marine ingress objects in the field. Despite this restriction, due to the comparative nature of this work, the inclusion of this heterogeneity is not essential. Ingress object drift is another notable exclusion within the simulated blooms and flights, however in the context of the duration of UAS flights (commonly between 30 and 60 mins (Mesas-Carrascosa et al., 2015, 2016; Sherstjuk, Zharikova and Sokol, 2018)), and the slow rate of surface and subsurface object drift (Li et al., 2019), it was deemed not constructive to the overall simulation. When randomised over thousands of iterations, whereby drift effects would result in an equivalent impact on detection capability across-the-board or oppose each other and culminate in a cancelling effect. This is a consequence of the symmetrical nature of the investigated survey patterns and would not be the case for asymmetrical search patterns. The simulations also follow the assumption of 100% successful detection of marine ingress objects within the field of view of

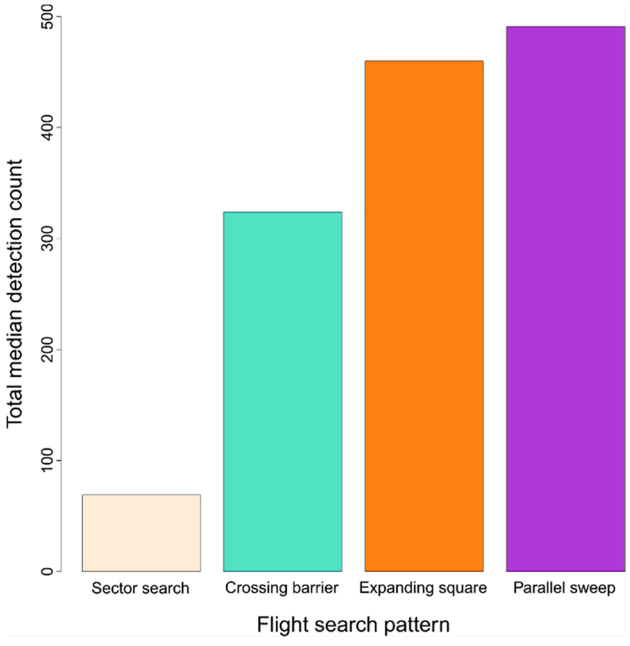


Fig. 9. Overall search style performance on all five forms of investigated bloom.

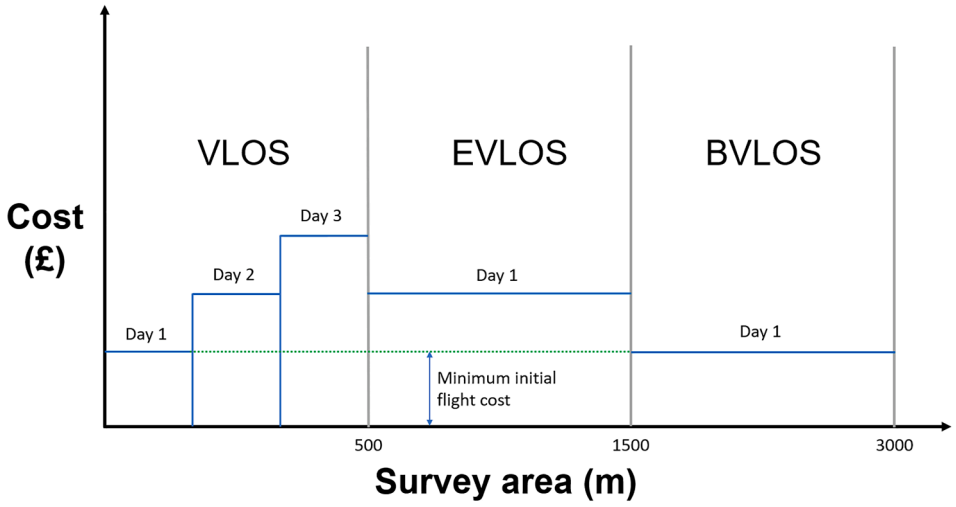


Fig. 10. Indicative relationship between financial cost of operation and increase in maximum theoretical survey area. Maximum distance for BVLOS is just indicative.

the UAS imaging system. In the field this would not be the case, however for the purpose of this work, the importance lies in consistency for legitimate comparison. The discrimination of the different types of marine ingress is an important feature by any early warning system. Despite it not being a focus of this work, it is still worth mentioning that any algorithms developed for the real-world detection of marine ingress should be able to cope with multiple forms of ingress; be it jellyfish or macroalgaes. Other minor forms of marine ingress that don't cause significant issues such as silverfish would not be worth attempting to detect due to the lack of disruption they can cause to coastal operators. The ability to discriminate between various forms of problematic macroalgaes was conducted by Mcilwaine et al. (2019) and it would be worthwhile for further research to investigate jellyfish in the same manner.

The production of a decision chart (Fig. 11) is a step towards a functioning early warning marine ingress detection system. At this

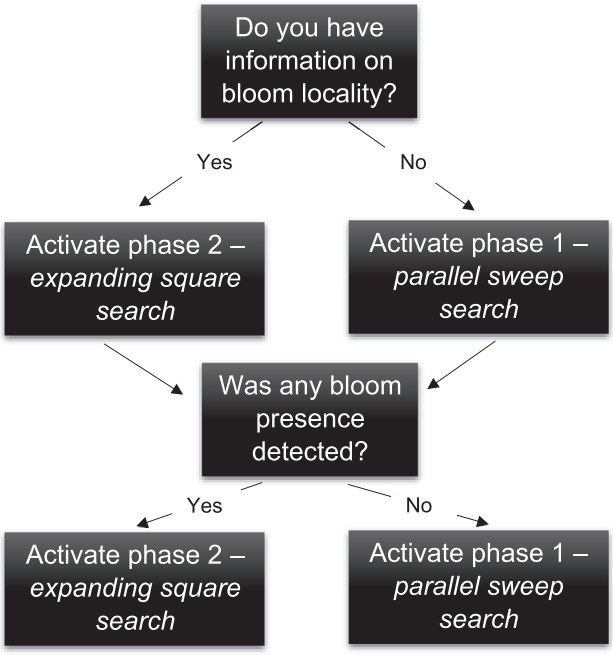


Fig. 11. Decision chart for UAS deployment for an established operation type (VLOS, EVLOS and BVLOS).

current time, there has been no work identifying optimal flight plans in the marine environment for marine ingress using UAS remote sensing. Coastal operators currently work off meteorological correlation risk-based systems, and if moving to positively identified ingress blooms using UAS remote sensing, they deserve clarity on what flight parameters to be using.

A field investigation that would be of interest would be to assess which flight pattern (over 1,000 s of flights) detects a bloom quickest. This was not a focus of this work but would be complementary to investigate building on the findings of this paper. Further work to build on this paper would be to investigate the impacts of various platform features on bloom detection, such as: flight speed, flight heights and the associated field of view changes, and the resolution of the on-board sensor. A similar investigation into the effect of environmental conditions would be equally enlightening. Particularly, the variation in detection performance due to change in wind direction/strength and the reduction/gain of flight duration as a result. By moving towards a standardised framework for marine ingress detection, the overall performance of detection and the ability to prevent losses of generation (or revenue for non-power station coastal industries) gradually increases. With a deployable finished framework that can account for many more flight parameters, the impact of problematic marine ingress bloom events should reduce to a much more manageable level when used in tandem with effective mitigation measures once a warning has been provided. No real-world testing of the simulation findings was carried out due to the immense difficulty of finding real-world blooms to test the various strategies on. However, there are no indications from the simulations (or the logic therein) that would dramatically impact overall flight performance in comparison to one another. To build on the work described in this paper, the authors recommend further investigation into encompassing more variables in their simulations. Investigation into the effects of differing ground sampling distance, wind buffeting and battery endurance would be worthy of consideration. The real-world deployment of the strategies discussed in this article would be of valuable contribution to knowledge as well, to ground-truth the findings of the extensive simulations conducted. There are situations in which marine ingress may occur in both forms of jellyfish and macroalgae. It would be prudent to build on the work conducted by Mcilwaine and Rivas Casado (2021) in order to add macroalgae detection classes into the detection algorithm so that both forms of marine ingress can be detected using the same single discrimination algorithm.

This work delivers the assessment for quantifying the optimal flight search patterns for marine ingress detection in the context of using UAS as a remote sensing platform. Within the context of moving towards a

functional early warning system for marine ingress, it is hoped that the provision of reliable early warning can aid coastal industries in preventing unnecessary losses and downtime from disruptive blooms (Hamner and Dawson, 2009). Examples of such preventative measures are protective aquatic barrier curtains (Zielinski and Sorensen, 2016), increased labour force for manual washing of filtration systems and preemptive reductions in water intake to prevent longer-term disruption (Nuclear Energy Institute, 2015; Wei et al., 2018). Through the introduction of this paper's findings, losses due to the impacts of marine ingress should hopefully be reduced. Future projects are recommended to investigate the current state of UAS technology, and what final steps are required to attain a fully functioning marine ingress early warning system. This is particularly crucial due to how rapidly this field of research is advancing on a yearly basis (Davies et al., 2018). The current global trend is an increase in disruptive ingress events, in both the two most common forms; jellyfish (Mills, 2001) and MABs (Spanakis et al., 2014). For our global coastal industries not to suffer further, especially in the post-COVID-19 era of extreme economic uncertainty (Baker et al., 2020), it should be a key priority to react proactively to these hazards and not reactionarily.

5. Conclusion

After completing a total of 50,000 simulations, the outputs showed a clear result in which flight search pattern was both the highest performer, but also most consistent for detecting marine ingress. Parallel sweep was the best performing flight search pattern, closely followed by expanding square. These were coincidentally a phase one and phase two flight search pattern respectively. It was also found that type of flight operation had a significant impact on marine ingress detection, with performance improvements (over VLOS) of 94% for EVLOS and 269% for BVLOS for a comparable density bloom but increased maximum theoretical survey area. With regard to bloom shape, large coverage blooms were the hardest to detect with circular blooms the easiest. The field testing of the findings of these simulations is recommended, as well as progressing the complexity of simulations if there is a demand to do so. With the occurrence of marine ingress blooms notably increasing around the globe, the effects of global changes are becoming more and more apparent. Thus, it is vital to continue this line of research if we are to maintain functionality and maximise the operational capacity of key coastal industries; particularly aquaculture, desalination plants and nuclear power stations. The impact of improving our understanding of marine ingress events is wide-ranging and will likely become increasingly important if we are to achieve our COP26 carbon neutrality agreements. Especially with nuclear power being the foundation of a reliable low-carbon energy economy.

Funding

This research was funded by the Engineering and Physical Sciences Research Council (EPSRC), The Smith Institute and EDF Energy under EPSRC Industrial Case Studentship Voucher 586 Number 16000001.

CRediT authorship contribution statement

Ben Mcilwaine: Methodology, Software, Validation, Investigation, Data curation, Writing – original draft, Writing – review & editing. **Mónica Rivas Casado:** Writing – review & editing, Supervision, Project administration, Funding acquisition. **Toby Waine:** Writing – review & editing, Supervision.

Declaration of Competing Interest

The authors declare the following financial interests/personal relationships which may be considered as potential competing interests: [Monica Rivas Casado reports financial support was provided by Engineering and Physical Sciences Research Council. Monica Rivas Casado reports financial support was provided by EDF Energy.]

Acknowledgements

We would like to thank the Engineering and Physical Sciences Research Council (EPSRC), The Smith Institute and EDF Energy for funding this project. We would also like to thank the reviewers for their helpful comments and constructive criticism. The manuscript became stronger thanks to their detailed contribution. The underlying data are confidential and cannot be shared due to a permanent embargo.

References

Albajes-Eizagirre, A., 2011. Jellyfish prediction of occurrence from remote sensing data and a non-linear pattern recognition approach. In: Neale, C.M.U., Maltese, A. (Eds.), International Society for Optics and Photonic, p. 817418. https://doi.org/10.1117/12.898162.

APA, 2020. Drones: Flying toward the future. Available at: APA Planning Advisory Service Reports 2020 (597), 1–109 https://www.scopus.com/inward/record.url?eid=2-s2.0-85098713055&partnerID=40&md5=6940cfcc04d807f827d1bccb228c8776.

Auditorium, S., Washington, D. C., 1980. BSÜE Visual Search Techniques Proceedings of a Symposium Sponsored by the ARMED FORCES-NRC COMMITTEE ON VISION.

Baker, S.R. et al., 2020. 'COVID-Induced Economic Uncertainty'. Available at: http://www.worlduncertaintyindex.com, (Accessed: 9 July 2021).

Barath Kumar, S., et al., 2017. Impingement of marine organisms in a tropical atomic power plant cooling water system. Mar. Pollut. Bull. 124 (1), 555–562. https://doi.org/10.1016/j.marpolbul.2017.07.067.

Becking, L.E., de Leeuw, C., Vogler, C., 2015. Newly discovered "jellyfish lakes" in Misool, Raja Ampat, Papua, Indonesia. Mar. Biodivers. 45 (4), 597–598. https://doi.org/10.1007/s12526-014-0268-6.

Benassi, F., et al., 2017. Testing Accuracy and Repeatability of UAV Blocks Oriented with GNSS-Supported Aerial Triangulation. Remote Sens. 9 (2), 172. https://doi.org/10.3390/RS9020172.

Bricelj, V.M., et al., 2012. 'Trophic transfer of brevetoxins to the benthic macrofaunal community during a bloom of the harmful dinoflagellate Karenia brevis in Sarasota Bay, Florida. Harmful Algae 16, 27–34. https://doi.org/10.1016/j.hal.2012.01.001.

CAA, 2021a. Airspace change proposal public view. Available at: https://airspacechange.caa.co.uk/PublicProposalArea?pID=385 (Accessed: 3 December 2021).

CAA, 2021b. Step forward for the drone industry as Civil Aviation Authority authorises trial of a concept for routine BVLOS operations | UK Civil Aviation Authority. Available at: https://www.caa.co.uk/News/Step-forward-for-the-drone-industry-as–Civil-Aviation-Authority-authorises-trial-of-a-concept–for-routine-BVLOS-operations/ (Accessed: 9 July 2021).

Catapult, 2020. UK Drones Pathfinder Programme has a new pathfinder announced. Available at: https://cpold.catapult.org.uk/2020/07/22/uk-drones-pathfinder-programme-focusing-on-early-detection-of-marine-activity/ (Accessed: 9 July 2021).

Chae, J., et al., 2008. Distribution of a pelagic tunicate Salpa fusiformis in warm surface current of the eastern Korean waters and its impingement on cooling water intakes of Uljin nuclear power plant. J. Environ. Biol. 29 (4), 585–590.

Civil Aviation Authority, 2020. Unmanned Aircraft System Operations in UK Airspace – Guidance. Crawley. Available at: https://publicapps.caa.co.uk/docs/33/CAP722Edition8(p).pdf (Accessed: 4 March 2021).

Colomina, I., Molina, P., 2014. Unmanned aerial systems for photogrammetry and remote sensing: A review. ISPRS J. Photogramm. Remote Sens. 79–97. https://doi.org/10.1016/j.isprsjprs.2014.02.013.

Davies, L., et al., 2018. Review of Unmanned Aircraft System Technologies to Enable beyond Visual Line of Sight (BVLOS) Operations. In: 2018 10th International Conference on Electrical Power Drive Systems, ICEPDS 2018 - Conference Proceedings, pp. 1–6. https://doi.org/10.1109/ICEPDS.2018.8571665.

Decker, M., et al., 2007. Predicting the distribution of the scyphomedusa Chrysaora quinquecirrha in Chesapeake Bay. Mar. Ecol. Prog. Ser. 329, 99–113. https://doi.org/10.3354/meps329099.

Dierssen, H.M., Chlus, A., Russell, B., 2015. Hyperspectral discrimination of floating mats of seagrass wrack and the macroalgae Sargassum in coastal waters of Greater Florida Bay using airborne remote sensing. Remote Sens. Environ. 167, 247–258. https://doi.org/10.1016/j.rse.2015.01.027.

Flynn, K., Chapra, S., 2014. Remote Sensing of Submerged Aquatic Vegetation in a Shallow Non-Turbid River Using an Unmanned Aerial Vehicle. Remote Sens. (12), 12815–12836. https://doi.org/10.3390/rs61212815.

Gansel, L.C., et al., 2017. Drag on nets fouled with blue mussel (mytilus edulis) and sugar kelp (saccharina latissima) and parameterization of fouling. In: Proceedings of the International Conference on Offshore Mechanics and Arctic Engineering - OMAE. American Society of Mechanical Engineers (ASME). https://doi.org/10.1115/OMAE201762030.

Goebel, M.E., et al., 2015. A small unmanned aerial system for estimating abundance and size of Antarctic predators. Polar Biol. 38 (5), 619–630. https://doi.org/10.1007/s00300-014-1625-4.

Gonçalves, G., et al., 2020. Quantifying marine macro litter abundance on a sandy beach using unmanned aerial systems and object-oriented machine learning methods. Remote Sensing 12 (16). https://doi.org/10.3390/RS12162599.

Haberlin, D., McAllen, R., Doyle, T.K., 2021. Field and flume tank experiments investigating the efficacy of a bubble curtain to keep harmful jellyfish out of finfish pens. Aquaculture 531. https://doi.org/10.1016/j.aquaculture.2020.735915.
Hamner, W., Dawson, M., 2009. A review and synthesis on the systematics and evolution of jellyfish blooms: Advantageous aggregations and adaptive assemblages. Hydrobiologia 616 (1), 161–191. https://doi.org/10.1007/s10750-008-9620-9.
Hayes, E.H., Landis, W.G., 2004. Regional ecological risk assessment of a near shore marine environment: Cherry Point, WA. Hum. Ecol. Risk Assess. 10 (2), 299–325. https://doi.org/10.1080/10807030490438256.
Houghton, J., et al., 2006. Developing a simple, rapid method for identifying and monitoring jellyfish aggregations from the air. Mar. Ecol. Prog. Ser. 314, 159–170. https://doi.org/10.3354/meps314159.
Hu, C., Muller-Karger, F.E., Swarzenski, P.W., 2006. Hurricanes, submarine groundwater discharge, and Florida's red tides. Geophys. Res. Lett. 33 (11) https://doi.org/10.1029/2005GL025449.
Jo, Y.-H., Bi, H., Lee, J., 2017. Potential Applications of Low Altitude Remote Sensing for Monitoring Jellyfish. Korean J. Remote Sens. 33 (1), 15–24. https://doi.org/10.7780/kjrs.2017.33.1.2.
Kim, D.H., et al., 2012. Estimating the economic damage caused by jellyfish to fisheries in Korea. Fish. Sci. 78 (5), 1147–1152. https://doi.org/10.1007/s12562-012-0533-1.
Kim, H., et al., 2015. Development of a UAV-type jellyfish monitoring system using deep learning. In: 2015 12th International Conference on Ubiquitous Robots and Ambient Intelligence (URAI). IEEE, pp. 495–497. https://doi.org/10.1109/URAI.2015.7358813.
Kim, H., et al., 2016. Image-based monitoring of Jellyfish using deep learning architecture. IEEE Sensors J. 16 (8), 2215–2216. https://doi.org/10.1109/JSEN.2016.2517823.
Klebert, P., et al., 2013. Hydrodynamic interactions on net panel and aquaculture fish cages: A review. Ocean Eng. 260–274. https://doi.org/10.1016/j.oceaneng.2012.11.006.
Kwon, Y.S., et al., 2020. Drone-based hyperspectral remote sensing of cyanobacteria using vertical cumulative pigment concentration in a deep reservoir. Remote Sens. Environ. 236 https://doi.org/10.1016/j.rse.2019.111517.
Lapointe, B.E., Bedford, B.J., 2007. Drift rhodophyte blooms emerge in Lee County, Florida, USA: Evidence of escalating coastal eutrophication. Harmful Algae 6 (3), 421–437. https://doi.org/10.1016/J.HAL.2006.12.005.
Li, D., et al., 2019. 'Characteristics and influence of green tide drift and dissipation in Shandong Rongcheng coastal water based on remote sensing', *Estuarine*. Coastal and Shelf Science 227, 106335. https://doi.org/10.1016/J.ECSS.2019.106335.
Li, L., Wu, J., 2021. Spatiotemporal estimation of satellite-borne and ground-level NO2 using full residual deep networks. Remote Sens. Environ. 254 https://doi.org/10.1016/j.rse.2020.112257.
Lippmann, J.M., et al., 2011. Fatal and severe box jellyfish stings, including Irukandji stings, in Malaysia, 2000–2010. J. Travel Med. 18 (4), 275–281. https://doi.org/10.1111/j.1708-8305.2011.00531.x.
Liu, G., et al., 2020. A new biomimetic antifouling method based on water jet for marine structures. Proc. Inst. Mech. Eng. Part M: J. Eng. Maritime Environ. 234 (2), 573–584. https://doi.org/10.1177/1475090219892420.
Di Luca, M., et al., 2020. A bioinspired Separated Flow wing provides turbulence resilience and aerodynamic efficiency for miniature drones. Sci. Robot. 5 (38) https://doi.org/10.1126/SCIROBOTICS.AAY8533/SUPPL_FILE/AAY8533_SM.PDF.
Maclsaac, H.J., 1996. Potential abiotic and biotic impacts of zebra mussels on the inland waters of North America. Am. Zool. 36 (3), 287–299. https://doi.org/10.1093/icb/36.3.287.
Mardones, J.I., et al., 2021. Disentangling the environmental processes responsible for the world's largest farmed fish-killing harmful algal bloom: Chile, 2016. Sci. Total Environ. 766 https://doi.org/10.1016/j.scitotenv.2020.144383.
Marx, U.C., Roles, J., Hankamer, B., 2021. Sargassum blooms in the Atlantic Ocean – From a burden to an asset. Algal Res. 54, 102188. https://doi.org/10.1016/j.algal.2021.102188.
Matsumura, K., et al., 2005. Genetic polymorphism of the adult medusae invading an electric power station and wild polyps of Aurelia aurita in Wakasa Bay, Japan. J. Mar. Biol. Assoc. U. K. 85 (3), 563–568. https://doi.org/10.1017/S0025315405011483.
Mcilwaine, B., Rivas Casado, M., 2021. JellyNet: The convolutional neural network jellyfish bloom detector. Int. J. Appl. Earth Obser. Geoinformation 97, 102279. https://doi.org/10.1016/j.jag.2020.102279.
Mcilwaine, B., Rivas Casado, M., Leinster, P., 2019. Using 1st Derivative Reflectance Signatures within a Remote Sensing Framework to Identify Macroalgae in Marine Environments. Remote Sensing 11 (6), 704. https://doi.org/10.3390/rs11060704.
Menu, M., et al., 2021. Towards a better understanding of grass bed dynamics using remote sensing at high spatial and temporal resolutions. Estuarine Coastal Shelf Sci. 251, 107229. https://doi.org/10.1016/j.ecss.2021.107229.
Mesas-Carrascosa, F.-J., et al., 2015. (2015) Assessing Optimal Flight Parameters for Generating Accurate Multispectral Orthomosaicks by UAV to Support Site-Specific Crop Management. Remote Sens. 7 (10), 12793–12814. https://doi.org/10.3390/RS71012793.
Mesas-Carrascosa, F.-J., et al., 2016. An Analysis of the Influence of Flight Parameters in the Generation of Unmanned Aerial Vehicle (UAV) Orthomosaicks to Survey Archaeological Areas. Sensors 16 (11), 1838. https://doi.org/10.3390/S16111838.
Mills, C.E., 2001. 'Jellyfish blooms: are populations increasing globally in response to changing ocean conditions? Hydrobiologia 451 (1), 55–68. https://doi.org/10.1023/A:1011888006302.
Minamoto, T., et al., 2017. Environmental DNA reflects spatial and temporal jellyfish distribution. PLoS ONE. https://doi.org/10.1371/journal.pone.0173073.
Mohd-Din, M., et al., 2020. Prolonged high biomass diatom blooms induced formation of hypoxic-anoxic zones in the inner part of Johor Strait. Environ. Sci. Pollut. Res. 27 (34), 42948–42959. https://doi.org/10.1007/s11356-020-10184-6.
Nahirnick, N.K., et al., 2019. Mapping with confidence; delineating seagrass habitats using Unoccupied Aerial Systems (UAS). Remote Sens. Ecol. Conservat. 5 (2), 121–135. https://doi.org/10.1002/rse2.98.
Nuclear Energy Institute, 2015. Economic Impacts of The R.E. Ginna Nuclear Power Plant An Analysis by the Nuclear Energy Institute. Available at: http://www.nei.org (Accessed: 10 January 2019).
Panagiotou, P., Yakinthos, K., 2020. Aerodynamic efficiency and performance enhancement of fixed-wing UAVs. Aerosp. Sci. Technol. 99, 105575. https://doi.org/10.1016/J.AST.2019.105575.
Purcell, J.E., 2005. Climate effects on formation of jellyfish and ctenophore blooms: a review. J. Mar. Biol. Assoc. U. K. 85 (3), 461–476. https://doi.org/10.1017/S0025315405011409.
R Core Team, 2017. R: A language and environment for statistical computing. Vienna, Austria. Available at: https://www.r-project.org/.
Riascos, J.M., et al., 2018. Floating nurseries? Scyphozoan jellyfish, their food and their rich symbiotic fauna in a tropical estuary. PeerJ. 2018 (6) https://doi.org/10.7717/peerj.5057.
Rogozovsky, I., et al., 2021. Impact of aerosol layering, complex aerosol mixing, and cloud coverage on high-resolution MAIAC aerosol optical depth measurements: Fusion of lidar, AERONET, satellite, and ground-based measurements. Atmos. Environ. 247 https://doi.org/10.1016/j.atmosenv.2020.118163.
Rowan, G.S.L., Kalacska, M., 2021. A Review of Remote Sensing of Submerged Aquatic Vegetation for Non-Specialists. Remote Sens. 13 (4), 623. https://doi.org/10.3390/rs13040623.
Royal National Lifeboat Institution, 2017. Maritime Search and Rescue Manual. Poole. Available at: https://rnli.org/-/media/rnli/downloads/maritime-sar-2017.pdf.
Schaub, J., et al., 2018. Using unmanned aerial vehicles (UAVs) to measure jellyfish aggregations. Marine Ecol. Progress Series 591, 29–36. https://doi.org/10.3354/meps12414.
Sherstjuk, V., Zharikova, M., Sokol, I., 2018. Forest Fire-Fighting Monitoring System Based on UAV Team and Remote Sensing. In: 2018 IEEE 38th International Conference on Electronics and Nanotechnology, ELNANO 2018 - Proceedings. Institute of Electrical and Electronics Engineers Inc., pp. 663–668. https://doi.org/10.1109/ELNANO.2018.8477527
Simic Milas, A., et al., 2018. Unmanned Aerial Systems (UAS) for environmental applications special issue preface. Int. J. Remote Sens. 4845–4851. https://doi.org/10.1080/01431161.2018.1491518.
Slidetodoc, 2021. Search Patterns W S Objectives DEMONSTRATE search pattern. Available at: https://slidetodoc.com/search-patterns-w-s-objectives-demonstrate-search-pattern/ (Accessed: 9 July 2021).
Sony, 2021. ILCE-6000 / ILCE-6000L / ILCE-6000Y / ILCE-6000Z Specifications | Cameras | Sony UK. Available at: https://www.sony.co.uk/electronics/interchangeable-lens-cameras/ilce-6000-body-kit/specifications (Accessed: 16 November 2021).
Spanakis, N., et al., 2014. Modelling of seaweed ingress into a nuclear power station cooling water intake. In: 21st TELEMAC MASCARET User Conference, pp. 125–131.
Thompson, T.M., Young, B.R., Baroutian, S., 2020. Pelagic Sargassum for energy and fertiliser production in the Caribbean: A case study on Barbados. Renew. Sustain. Energy Rev. https://doi.org/10.1016/j.rser.2019.109564.
Thomsen, P.F., et al., 2012. Detection of a Diverse Marine Fish Fauna Using Environmental DNA from Seawater Samples. PLoS ONE 7 (8), e41732. https://doi.org/10.1371/journal.pone.0041732.
Thorn, A., Lambert, N., 2016. Workshop: Managing Ocean risks (Satellites for managing ocean risks). Available at: https://sa.catapult.org.uk/south-coast/wp-content/uploads/sites/6/2016/09/MOR_23-Sep-2016_Combined-Presentations-less-ASV-3.pdf (Accessed: 11 May 2020).
Tombs, R., Radford, U., 2015. ADW: Aurelia aurita: INFORMATION. Available at: https://animaldiversity.org/accounts/Aurelia_aurita/ (Accessed: 5 July 2021).
Vasslides, J.M., Sassano, N.L., Hales, L.S., 2018. Assessing the effects of a barrier net on jellyfish and other local fauna at estuarine bathing beaches. Ocean Coastal Manage. 163, 364–371. https://doi.org/10.1016/j.ocecoaman.2018.07.012.
Vaughan, A., 2018. In a laver: seaweed shuts nuclear reactor again in bad weather | Business | The Guardian, The Guardian. Available at: https://www.theguardian.com/business/2018/mar/05/seaweed-shuts-nuclear-reactor-edf-torness-plant (Accessed: 22 February 2019).
Ventura, D., et al., 2018. Mapping and classification of ecologically sensitive marine habitats using unmanned aerial vehicle (UAV) imagery and Object-Based Image Analysis (OBIA). Remote Sens. 10 (9) https://doi.org/10.3390/rs10091331.
Wei, M., et al., 2018. Early warning model for marine organism detection in nuclear power stations. In: Proceedings of the 30th Chinese Control and Decision Conference, CCDC 2018. Institute of Electrical and Electronics Engineers Inc., pp. 1999–2004. https://doi.org/10.1109/CCDC.2018.8407454
Weybright, S., Kelly, P., 2016. Algal bloom turns ocean red. In: OCEANS 2015 - MTS/IEEE Washington. Institute of Electrical and Electronics Engineers Inc. https://doi.org/10.23919/oceans.2015.7404622
Zhu, H., et al., 2020. Design and assessment of octocopter drones with improved aerodynamic efficiency and performance. Aerosp. Sci. Technol. 106, 106206. https://doi.org/10.1016/J.AST.2020.106206.
Zielinski, D.P., Sorensen, P.W., 2016. Bubble Curtain Deflection Screen Diverts the Movement of both Asian and Common Carp. North Am. J. Fish. Manag. 36 (2), 267–276. https://doi.org/10.1080/02755947.2015.1120834.
Zoltan, T.B., Taylor, K.S., Achar, S.A., 2005. Health issues for surfers. Am. Fam. Physician.



https://dspace.org/

Investigating optimal unmanned aircraft systems flight plans for the detection of marine ingress

Mcilwaine, Ben; Rivas Casado, Monica; Waine, Toby W.

2022-03-08
Elsevier
https://doi.org/10.1016/j.jag.2022.102729
Mcilwaine B, Rivas Casado M, Waine T. (2022) Investigating optimal unmanned aircraft systems flight plans for the detection of marine ingress, International Journal of Applied Earth Observation and Geoinformation, Volume 108, April 2022, Article number 102729

Downloaded from a DSpace repository. https://dspace.org/